Article:
Wood, JM, Oseghale, CI, Cespedes, O et al. (2018) Control of ferromagnetic properties of $Ni_{80}Fe_{20}$ thin films by voltage-induced oxidation. Journal of Applied Physics, 124 (8). ARTN 085304. ISSN: 0021-8979

https://doi.org/10.1063/1.5045552

Control of ferromagnetic properties of $Ni_{80}Fe_{20}$ thin films by voltage-induced oxidation

J. M. Wood, C. I. Oseghale, O. Cespedes, M. Grell, and D. A. Allwood

Citation: Journal of Applied Physics **124**, 085304 (2018); doi: 10.1063/1.5045552
View online: https://doi.org/10.1063/1.5045552
View Table of Contents: http://aip.scitation.org/toc/jap/124/8
Published by the American Institute of Physics

Control of ferromagnetic properties of $Ni_{80}Fe_{20}$ thin films by voltage-induced oxidation

J. M. Wood,[1] C. I. Oseghale,[2] O. Cespedes,[3] M. Grell,[4] and D. A. Allwood[1]
[1]*Department of Materials Science and Engineering, University of Sheffield, Portobello Street, Sheffield S1 3JD, United Kingdom*
[2]*Department of Chemical and Biological Engineering, University of Sheffield, Portobello Street, Sheffield S1 3JD, United Kingdom*
[3]*School of Physics and Astronomy, E. C. Stoner Laboratory, University of Leeds, Leeds LS2 9JT, United Kingdom*
[4]*Department of Physics and Astronomy, University of Sheffield, Hounsfield Road, Sheffield S3 7RH, United Kingdom*

(Received 21 June 2018; accepted 9 August 2018; published online 24 August 2018)

We demonstrate large voltage-induced changes of magnetic properties in thin films of $Ni_{80}Fe_{20}$ (permalloy) when gated using an ionic liquid medium [1-ethyl-3-methylimidazolium bis(trifluoromethylsulfonyl)imide (EMIMTFSI)]. The coercivity and magnetic moment of 5 nm thick permalloy films could be reduced by 75% and 35%, respectively, by using applied voltages. These changes were partially restored by reversing the potential polarity. Electrochemical, time-course magnetometry and surface analysis measurements suggest that the voltage-induced changes are due to changes in the oxidation state at the surface of the film, causing a thinning of the permalloy layer. The control of soft magnetic properties with low voltages may be of use in tuneable devices. *Published by AIP Publishing*. https://doi.org/10.1063/1.5045552

I. INTRODUCTION

Active control of magnetic properties offers significant flexibility in devices such as memories and sensors. This has been demonstrated in multiferroic,[1–4] piezoelectric-magnetostrictrive composite,[5–7] ferromagnetic semiconductor,[8–10] and magnetic thin film[11–18] systems. The latter cases showed that it is possible to control ferromagnetic properties with voltage or electric field directly. Maruyama *et al.*[17] demonstrated the voltage control of magnetic anisotropy of Fe monolayers by using a polyimide/MgO bilayer as a dielectric material to create electric fields at the magnetic interface. Applying voltages of ±200 V caused a 39% change in the surface anisotropy, with negative voltages inducing a perpendicular magnetic anisotropy (PMA) in the film. This was attributed to a change in the occupancy of 3d electrons in the Fe adjacent to the MgO. Bauer *et al.*[12] showed that oxygen migration across a PMA GdO_x/Co interface could be controlled using voltage and heat treatments. This resulted in a significant drop in coercivity and entire loss of PMA after applying −4 V to the oxide layer, and complete reversibility after applying +4 V and heating to 100 °C. Again these effects were attributed to a change in magnetic anisotropy due to the oxygen ion presence. Electrolytes have also been used as an alternative to oxide dielectrics. Weisheit *et al.*[11] added Na^+ ions to propylene carbonate to generate electric fields of up to 4 GV.m^{-1} at the interface with FePt and FePd films. This induced changes of up to 4.5% in coercivity, attributed to a change in unpaired 3d electrons at the interface. Di *et al.*[19] used an electrochemical approach to vary the surface chemistry of a thin film of Co in aqueous KOH solution to achieve reversible voltage-induced changes in coercivity, magnetization, and surface anisotropy. The recent focus on using ionic liquids to create high electric fields at the magnetic interface has resulted in relatively low (<±5 V) applied voltages creating large changes in coercivity and magnetization of Fe, Ni, and Co films,[13–15] which has again been attributed to the control of oxidation conditions.

Permalloy ($Ni_{80}Fe_{20}$) is a popular material for use in thin films[20] and patterned structures.[21,22] Here we demonstrate the direct voltage control of coercivity and magnetic moment in permalloy thin films when part of an electrochemical cell made with the ionic liquid 1-ethyl-3-methylimidazolium bis(trifluoromethylsulfonyl)imide (EMIMTFSI). These changes in coercivity remained after voltage was removed, which shows a non-volatile change in the surface.

II. METHOD

Thin films of permalloy ($Ni_{80}Fe_{20}$) were thermally evaporated at a base pressure of 1×10^{-7} mbar onto a Si (100) substrate containing a native oxide. Sample dimensions were approximately 1 cm × 2 cm laterally and 5 nm in thickness, verified by atomic force microscopy (AFM; Veeco Nanoscope 3D Dimension 3100). The measurement cell (Fig. 1) consisted of two strips of Kapton® tape, 10 mm × 2 mm × 0.03 mm, placed onto the magnetic film to create an insulating barrier. 10–20 μL of EMIMTFSI (IOLITEC, 99%) was deposited between the Kapton strips using a syringe. EMIMTFSI was used as the ionic liquid because it has a large electrochemical window (ECW) of approximately 4.4 V,[23] which allows a wide range of voltages to be applied, and is known to be stable in air.[23] A transparent indium tin oxide (ITO)-coated glass slide was placed over

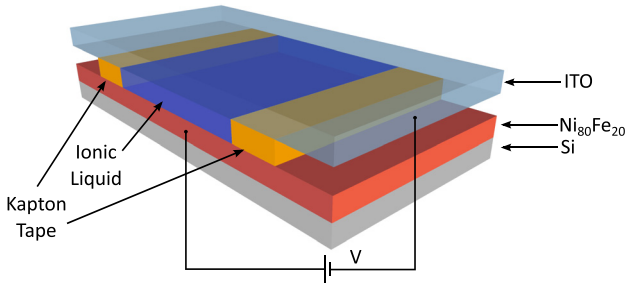

FIG. 1. Schematic of experimental cell consisting of a 5 nm thermally evaporated $Ni_{80}Fe_{20}$ film on Si substrate with the ionic liquid (EMIMTFSI) enclosed by two strips of Kapton® tape and an ITO-coated glass slide. Voltage is applied across the cell by electrical connections to the permalloy film and ITO-coated glass.

the assembly with the ITO contacting the ionic liquid to ensure optical access to the permalloy film.

Voltage was applied using the permalloy and ITO layers as electrodes, with the potential of the permalloy defined relative to the ITO. This created an electric double layer (EDL) at the magnetic film/ionic liquid interface generating a large electric field.[24] Magnetic hysteresis loops of the $Ni_{80}Fe_{20}$ films were obtained using longitudinal magneto-optical Kerr effect (MOKE) magnetometry, with 632 nm wavelength laser light. The coercivity, H_C, and switching behavior were obtained from hysteresis loops measured at a frequency of 6 Hz averaged over 500 loops (i.e., taking approximately 80 s overall). The cell was then dismantled and the thin films washed in isopropanol alcohol (IPA) to stabilize the surface against further action by the ionic liquid. Vibrating sample magnetometry (VSM; Quantum Design MPMS 3) was used to characterize the magnetic moment of the washed films. X-ray photoelectron spectroscopy (XPS; Thermo K-alpha) analyzed the surface properties of the washed thin films using 1486.6 eV X-ray beams with a 400 μm spot size and an electron pass energy of 200 eV. XPS measurements were made at room temperature in three positions on each sample and averaged. Cyclic voltammetry (CV) (Solartron Analytical 1400-1470E) was performed on cells consisting of two permalloy-coated Cu disks separated by the ionic liquid. Cyclic voltammograms were recorded by sweeping the potential in the anodic direction from the open-circuit potential to +2.5 V and then in the cathodic direction to −2.5 V and back to the starting potential, at a scan rate of 5 $mV.s^{-1}$.

III. RESULTS

Before exploring magnetic effects, it was important to establish the electrochemical nature of permalloy. Figure 2 shows a CV loop obtained using potentials between +2.5 V and −2.5 V until a stabilized CV characteristic was observed. The CV characteristic shows three anodic and three cathodic peak current densities: the first and primary anodic peak (oxidation reaction) appeared at +0.30 V with $J = 0.234\,mA.cm^{-2}$ (peak *a*); this was followed by two oxidation peaks at +1.76 V and +1.95 V (peaks *b* and *c*, respectively). In the reverse scan direction (reduction reaction), the three (negative-going) peaks appeared at +2.25 V, −0.23 V, and −1.81 V (peaks *d*, *e*, and *f*, respectively). The increased current density in the forward

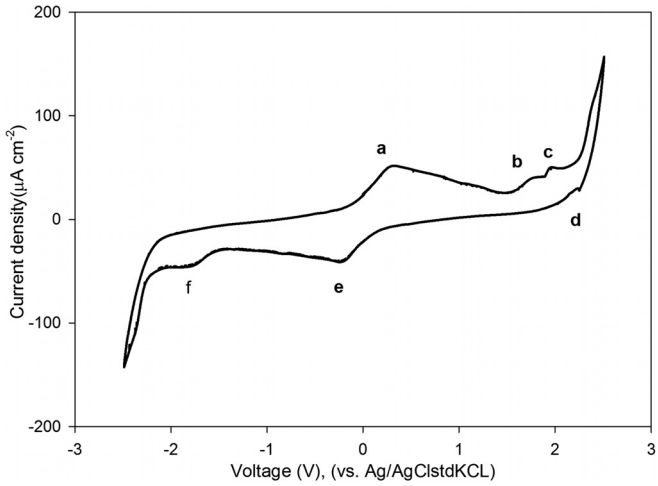

FIG. 2. Cyclic voltammogram of a Cu-permalloy-EMIMTFSI-permalloy-Cu cell between +2.5 V and −2.5 V, against a silver chloride reference electrode. Panels (a)–(f) identify significant peaks in the current density passing through the cell.

scan direction is due to the oxidation at the interface between the 1-ethyl-3-methylimidazolium [EMIM] group and the permalloy film, while the increase in the current density on the reverse scan is due to reduction of the interfacial species created in the forward scan.[25] The ECW of EMIMTFSI is the potential range where there is no oxidation or reduction, i.e., inert within this potential range (defined here as where the absolute current density, $|J|$ does not exceed 1 $mA.cm^{-2}$) and was calculated by subtracting the reduction potential limit from the oxidation potential limit.[23,25,26] The value of 4.4 V obtained for the ECW width here is in agreement with previous measurements.[23,25] In a further CV study where the applied voltage was only cycled between positive voltages and 0 V (no negative voltages), the current peak at +2.6 V was only present in the first cycle, which indicated a saturation of the oxidation process.

Magnetic hysteresis loops were taken from a single sample under a sequence of applied voltages of 0 V, +4 V, 0 V, and −4 V, with each applied for approximately 5 min before a hysteresis loop was obtained at each voltage. Hysteresis loops showed a significant decrease in coercivity when the voltage was increased to +4 V [Figs. 3(a) and 3(b)], while also showing a 2.5 times decrease in the Kerr signal. The coercivity and Kerr signal decreased further when the voltage was decreased to 0 V [the coercivity by 80% in Fig. 3(c) compared to original value]. When subsequently applying −4 V [Fig. 3(d)], the coercivity increased by 59% of the minimum value at 0 V [Fig. 3(c)]. At −4 V, the Kerr signal returned to a comparable value to that of +4 V. The simultaneous observed changes in coercivity and Kerr signal suggest a decrease in the thickness of the ferromagnetic film.

Measurements were repeated on fresh samples with smaller steps of 1 V up to a maximum positive voltage value of +3 V. Each voltage was applied for 2 min before the MOKE measurement was performed, apart from −4 V which was followed by MOKE measurements after 2, 4, 6, and 10 min. The voltage was then removed and the samples

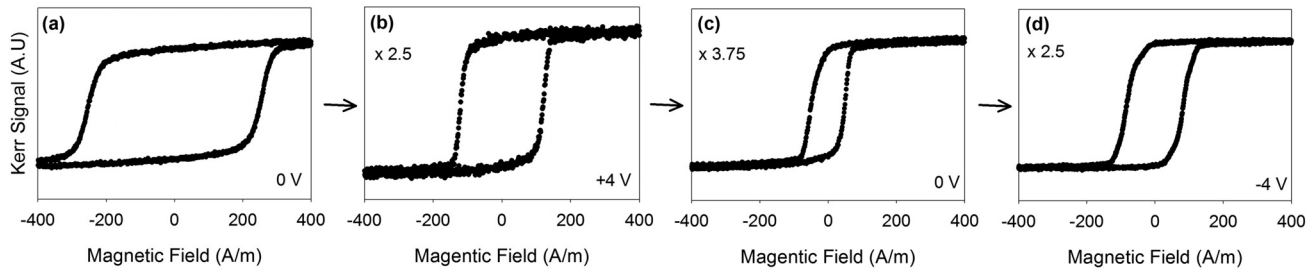

FIG. 3. MOKE-generated hysteresis loops of 5 nm permalloy film inside permalloy-EMIMTFSI-ITO cell under a sequence of voltages (a) 0 V, (b) +4 V, (c) 0 V, and (d) −4 V. Parts (b)–(d) also show the degree of signal enlargement applied to the data [compared to part (a)] for presentation purposes.

washed in IPA to stabilize the surface against further action by the ionic liquid before another MOKE measurement. The current through the cell was measured every 10 s throughout to give simultaneous cyclic voltammetry and MOKE magnetometry. Figure 4(a) shows similar results to Fig. 3, with a decrease in the coercivity of over 70% on the application of +3 V. The increase in measured current [Fig. 4(b)] at +3 V indicates an oxidative effect on the film, also demonstrated by CV plots in Fig. 2. On reversal of the voltage from +2 V to −2 V, there is little change in the coercivity and current, indicating that there is little chemical change. Application of −3 V saw a small increase in negative-going current and a slight increase in coercivity [Fig. 4(a)]. These effects increased upon application of −4 V and suggest a chemical reduction of the film. Maintaining the voltage at −4 V for a total of 10 minutes increased the coercivity to within 13% of its original value.

The MOKE hysteresis loops used to obtain coercivity in Fig. 4(a) were further analyzed to obtain the fractional Kerr signal $\Delta K/K_{ave}$, where ΔK and K_{ave} are the difference in Kerr signal and average Kerr signal in each loop, respectively. For the film thicknesses relevant here, $\Delta K/K_{ave}$ is proportional to changes in the relative magnetic moment.[27] Figure 4(c) shows that $\Delta K/K_{ave}$ follows a similar trend as coercivity to changes in the applied voltage, decreasing with the initial increasing positive voltage and then increasing again as the voltage polarity is reversed. The similarity of change in $\Delta K/K_{ave}$ and coercivity is less strong following the application of −4 V [Figs. 4(a) and 4(b)], with $\Delta K/K_{ave}$ only reaching approximately 50% of its initial value when returned to 0V.

The non-volatile nature of these voltage-dependent changes in coercivity and $\Delta K/K_{ave}$ suggests that the changes are due to redox reactions, as seen in previous similar studies of other materials.[12,28] The kinetics of the oxidation were investigated by performing MOKE magnetometry measurements under +1 V, +2 V, +3 V, and +4 V with hysteresis loops obtained at regular intervals. Figure 5 shows that the coercivity decreased at a higher rate for larger voltages, indicating faster oxidation. This means exposure time can also be used as a technique to control coercivity. However, the coercivity change is not a simple function of voltage and reflects the non-linear nature of electrochemistry present, as seen in the cyclic voltammogram in Fig. 2.

Thin films that had been subject to different voltages for 5 min and washed in IPA were characterized magnetically by VSM. All the samples that had a negative voltage applied were previously exposed to +3 V for 5 minutes. Figure 6(a) demonstrates a decrease in the magnetic moment per unit area for increasing positive voltage up to +3 V. The magnetic moment per unit area continued to decrease upon reversing voltage polarity up until −4 V where the magnetic

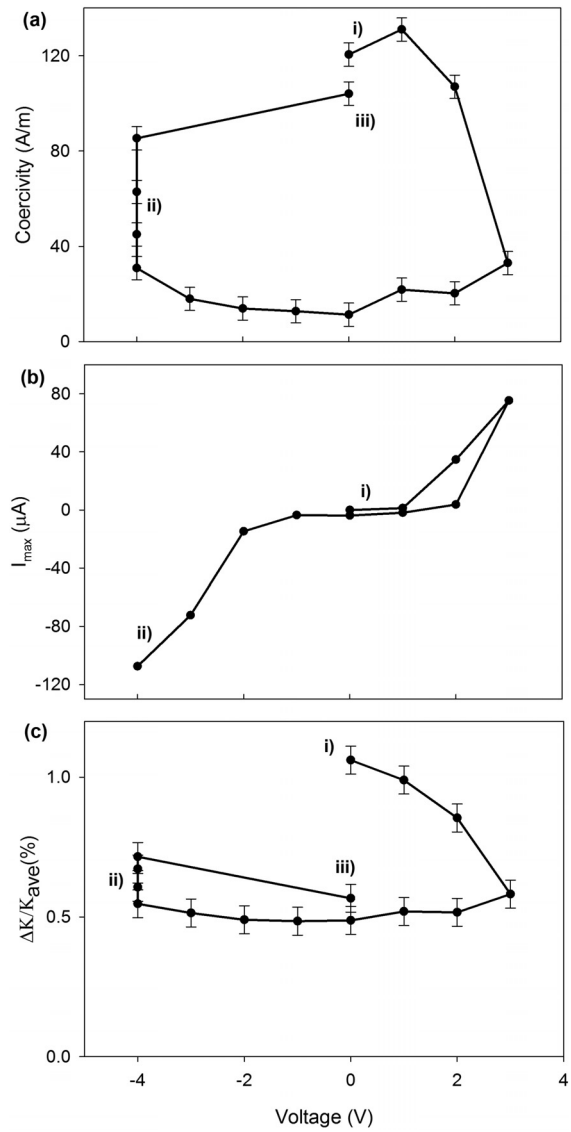

FIG. 4. (a) Coercivity of 5 nm permalloy film within a permalloy/EMIMTFSI/ITO cell as a function of voltage. (b) Maximum current passing through permalloy/EMIMTFSI/ITO cell at different applied voltages. (c) Fractional Kerr signal, $\Delta K/K_{ave}$, of 5 nm permalloy film as a function of voltage, while part of a permalloy/EMIMTFSI/ITO cell. (i) The start of the voltage sequence, 0 V. (ii) The cell remained for 10 min at −4 V and with measurements made at 2, 4, 6, and 10 min. (iii) The cell was dismantled, the permalloy film washed in IPA, and a final measurement made [so not shown in part (b)].

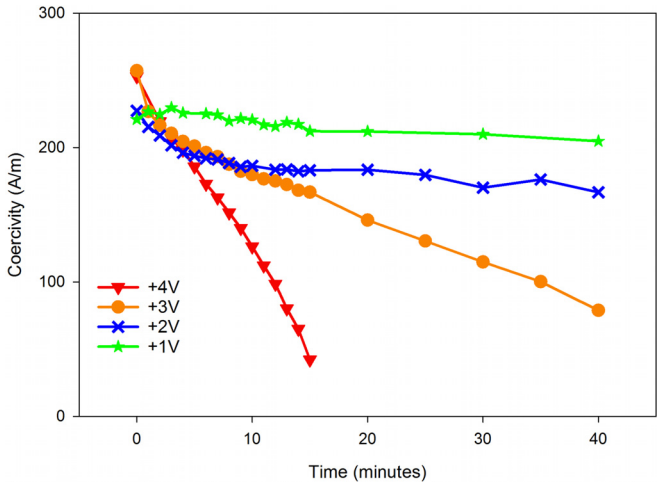

FIG. 5. Time course coercivity measurements of 5 nm permalloy films obtained from MOKE hysteresis loops, while exposed to +1 V, +2 V, +3 V, and +4 V, as part of permalloy/EMIMTFSI/ITO cell.

moment increased [Fig. 6(b)]. The coercivity measured from Figs. 6(a) and 6(b) showed a 60% decrease at +3 V and a subsequent increase at −4 V, following the same trend as MOKE coercivity (Figs. 3 and 4). It should be noted that the switching fields measured by VSM are less precise than MOKE in this study.

Calculation of magnetic moment per unit volume using a nominal initial film thickness of 5 nm produced reduced saturation magnetization values (M_S) for permalloy, even for unexposed samples, for which $M_S = 550$ kA/m was obtained. This could reflect a reduced thickness of ferromagnetic permalloy in the film due to native oxidation.[29] Calculation of the ferromagnetic thickness using $M_S = 800$ kA/m for permalloy[30] gave an initial ferromagnetic thickness of 3.4 nm. This correlates well with the observation of Fitzsimmons *et al.* of a 1.5 nm thick native oxide layer in permalloy films.[29] Figure 6(c) shows the variation of the ferromagnetic thickness with applied voltage, demonstrating a decrease in the film thickness with increasing voltage until −4 V was applied, when the ferromagnetic film thickness increased again. These voltage-induced magnetic layer thickness changes provide a simple explanation of the changes in MOKE measurements discussed above.

Thin films that had been subject to a voltage for 5 min and washed in IPA were analyzed using XPS, which probes 5–10 nm from the surface. All samples that had a negative voltage applied were previously exposed to +3 V for 5 min. The peak parameters for all spectra were fitted using data from Biesinger *et al.*[31,32] Figure 7(a) shows an example oxygen 1s energy peak from a permalloy film that had not been exposed to an applied voltage, following background subtraction and peak calibration to the C 1s peak. Deconvolution of the oxygen peak [Fig. 7(a)] shows components attributed to lattice oxides (529.5 eV), which are characteristic of permalloy oxidation,[33] hydroxide/lattice defects (531.5 eV), and water/organic species (533.7 eV). Fitzsimmons *et al.*[29] suggest that a NiO layer is present in permalloy films that have been exposed to air. Figure 7(b) shows the oxygen 1s peaks for all samples and Fig. 7(c) the

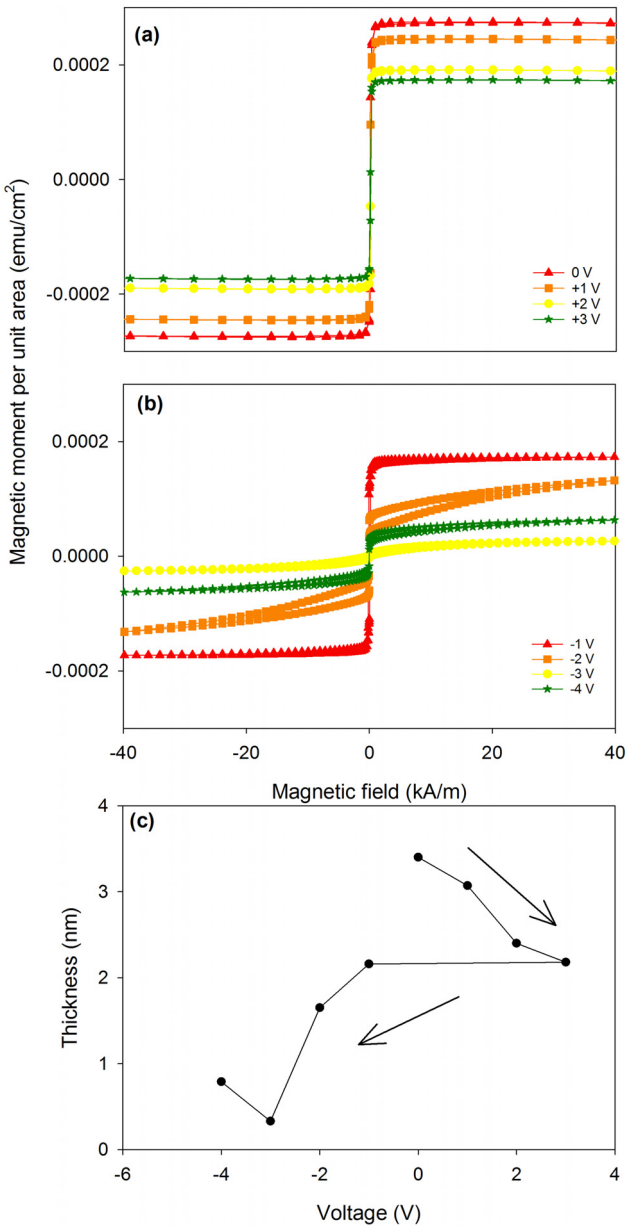

FIG. 6. VSM generated hysteresis loops showing magnetic moment per unit area of permalloy film as a function of applied field after exposure to a sequence of voltages while part of a permalloy/EMIMTFSI/ITO cell; all cells were dismantled and all films washed in IPA prior to VSM characterization. The voltage sequence passed from (a) 0 V to +3 V and subsequently to (b) −4V; all negative voltages had prior exposure to +3 V for 5 min. The reason for the different loop shape for the −2 V sample is unclear but does not affect the measurement of magnetic moment. (c) Reduced permalloy film thickness with applied voltage, calculated from reduced magnetic moment for 5 nm permalloy films observed in VSM data. Arrows indicate the direction of voltage sequence.

magnitude of the three peak components, with voltage plotted to follow the sequence in which it was applied. The lattice oxide peak remained unchanged until −3 V and −4 V, where it decreased. However, wide-energy survey spectra showed the appearance of In at −3 V and −4 V, thus covering the film and reducing the lattice oxide peak intensity. The water/organic species component decreased after +1 V, which is attributed to the electrolysis of water generating hydroxide ions. This is further supported by the increase in

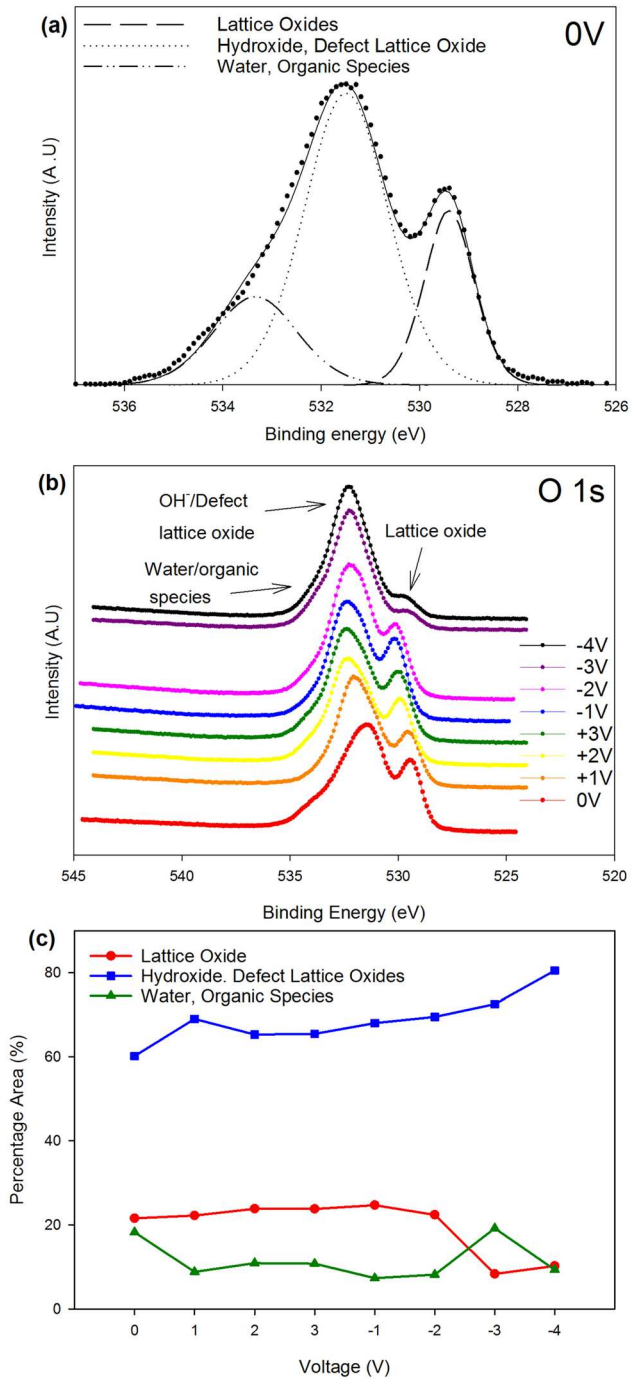

FIG. 7. (a) Deconvoluted XPS spectrum for O 1s energy range at 0 V and (b) XPS spectra for O 1s spectra for voltage range 0 V to +3 V to −4 V, arrows indicating lattice oxide species, hydroxide/defect lattice oxides and water/organic species, spectra have here been offset (c) change in the percentage area of O 1s components as a function of voltage.

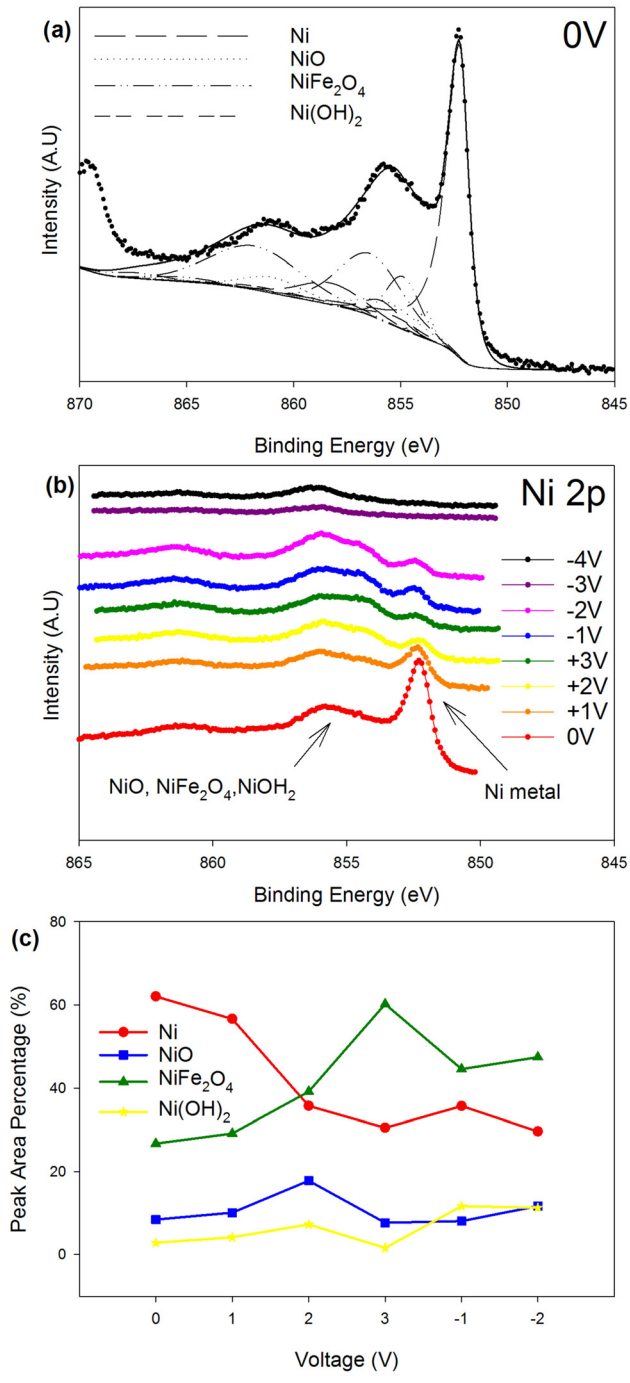

FIG. 8. (a) Deconvoluted XPS spectrum for Ni 2p energy range at 0 V and (b) XPS spectra for Ni 2p spectra for voltage range 0 V to +3 V to −4 V, arrows indicating a Ni metal peak and oxides/hydroxides, spectra have here been offset (c) change in the percentage area of Ni 2p components as a function of voltage.

hydroxide/defect lattice oxide components, a shift in peak position, and the minor peak at +0.3 V shown in CV data in Fig. 2.

Figure 8 shows the XPS data for the Ni 2p energy range, including example peak deconvolution of XPS for the 0 V Ni sample [Fig. 8(a)]. Fitting parameters from Biesinger *et al.*[32] were again used along with a Shirley background offset.[32] The sharp peak at 862.6 eV is attributed to Ni metal in the permalloy, while secondary peaks are attributed to NiO, $NiFe_2O_4$, and $Ni(OH)_2$ [Fig. 8(a)], further demonstrating the presence of an oxide layer above the permalloy at 0 V. Figures 8(b) and 8(c) show a decrease in the Ni metal peak with increasing positive voltage, while the Ni oxide and hydroxide peak grow, further suggesting a thinning of the Ni metal layer as the voltage increases.

Figure 9 shows the XPS spectra for the Fe 2p energy range, including deconvolution of the peak for the 0 V sample [Fig. 9(a)] and identification of contributions from Fe

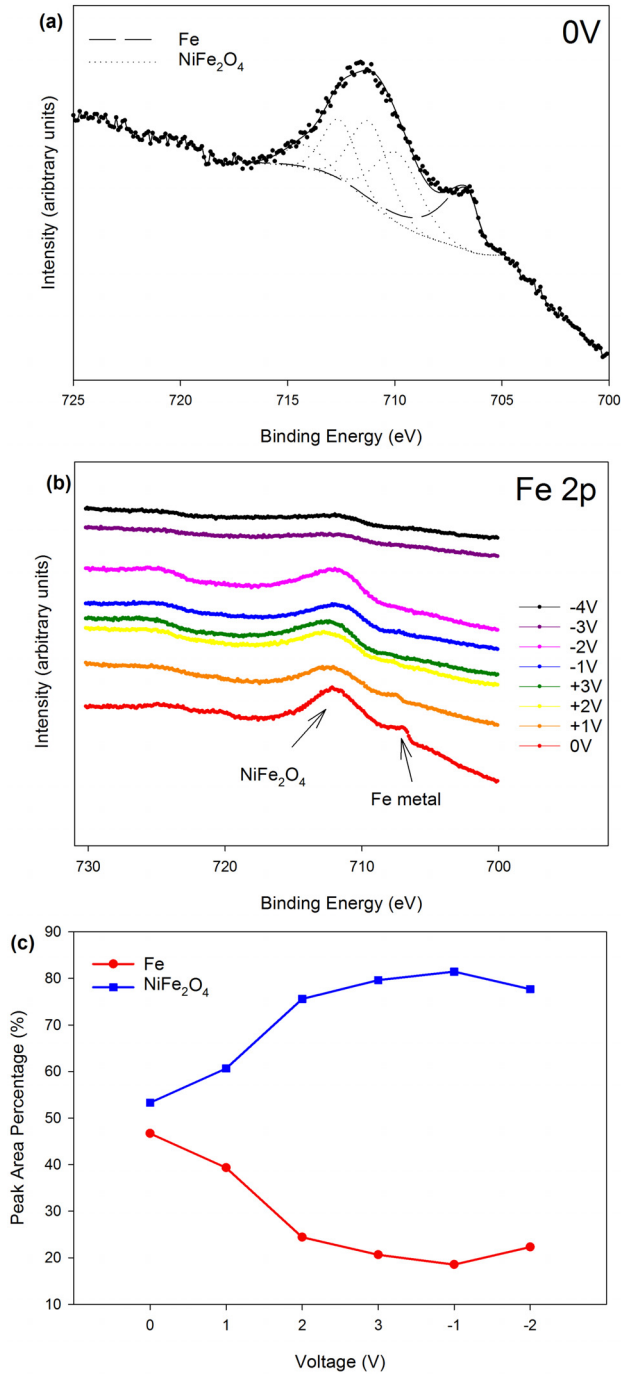

FIG. 9. (a) Deconvoluted XPS spectrum for Fe 2p energy range at 0 V (b) XPS spectra for Fe 2p spectra for voltage range 0 V to +3 V to −4 V, arrows indicating a Fe metal peak and NiFe2O4, spectra have here been offset (c) change in the percentage area of Fe 2p components as a function of voltage.

metal and $NiFe_2O_4$. No metal Fe peak was observed for samples above +2 V [Figs. 9(b) and 9(c)], with subsequent spectra showing only $NiFe_2O_4$, although In may again have masked any metal Fe in the −3 V and −4 V samples.

This agrees well with the observation of Fitzsimmons *et al.*[29] of a constant 1.5 nm layer of NiO on the permalloy surface after exposure to air, described above. Further, Fitzsimmons *et al.* show the formation of a 1 nm thick Fe-rich oxide layer directly beneath the NiO that increases in thickness with increasing oxidation. These reports are both consistent with the XPS data shown here. Thus, increasing positive voltage increases the thickness of the Fe-rich oxide, effectively thinning the permalloy layer and reducing the coercivity, relative magnetization, and magnetic moment.

The changes observed in XPS measurements concur with the cyclic voltammetry in suggesting significant oxidation of permalloy for voltages above +2 V. The resulting variation of ferromagnetic film thickness also explains the reversible changes in magnetic coercivity and magnetic moment observed in both MOKE and VSM data.

IV. SUMMARY

Large semi-reversible changes in coercivity, relative magnetization, and magnetic moment of permalloy thin films as part of an electrochemical cell containing the ionic liquid, EMIMTFSI, were observed upon application of voltage across the cell. XPS and cyclic voltammetry both showed that increasing positive voltages increased the degree of oxidation in the films. These increases in oxidation explain the observed changes in magnetic properties, due to changes in the thickness of the metallic permalloy. The rate of decrease in coercivity also increased with larger voltages, consistent with electrochemical processes. When a negative voltage is applied, the effect is reversed and the magnetic properties recovered substantially. The simple arrangement afforded by the electrolytic mediation of applied voltage offers flexibility in future tuneable magnetic structures. Future experiments could incorporate heat treatments[12] or wider exploration of voltage sequences and exposure times to improve the reversibility of magnetic properties.

ACKNOWLEDGMENTS

The authors would like to thank the team at the National EPSRC XPS Users' Service (NEXUS) for carrying out the XPS measurements and acknowledge EPSRC for a Ph.D. Studentship (Grant No. EP/I000933/1).

[1]Y. Tokunaga, Y. Taguchi, T. Arima, and Y. Tokura, Nat. Phys. **8**, 838 (2012).
[2]J. T. Heron, M. Trassin, K. Ashraf, M. Gajek, Q. He, S. Y. Yang, D. E. Nikonov, Y. H. Chu, S. Salahuddin, and R. Ramesh, Phys. Rev. Lett. **107**, 217202 (2011).
[3]D. Lebeugle, A. Mougin, M. Viret, D. Colson, and L. Ranno, Phys. Rev. Lett. **103**, 257601 (2009).
[4]S. M. Wu, S. A. Cybart, P. Yu, M. D. Rossell, J. X. Zhang, R. Ramesh, and R. C. Dynes, Nat. Mater. **9**, 756 (2010).
[5]J. W. Lee, S. C. Shin, and S. K. Kim, Appl. Phys. Lett. **82**, 2458 (2003).
[6]N. Lei, T. Devolder, G. Agnus, P. Aubert, L. Daniel, J.-V. Kim, W. Zhao, T. Trypiniotis, R. P. Cowburn, C. Chappert, D. Ravelosona, and P. Lecoeur, Nat. Commun. **4**, 1378 (2013).
[7]C. Thiele, K. Dörr, O. Bilani, J. Rödel, and L. Schultz, Phys. Rev. B **75**, 054408 (2007).
[8]D. Chiba, F. Matsukura, and H. Ohno, Appl. Phys. Lett. **89**, 162505 (2006).
[9]D. Chiba, M. Yamanouchi, F. Matsukura, and H. Ohno, Science **301**, 943 (2003).
[10]H. Ohno and H. Ohno, Nature **408**, 944 (2000).
[11]M. Weisheit, S. Fähler, A. Marty, Y. Souche, C. Poinsignon, and D. Givord, Science **315**, 349 (2007).
[12]U. Bauer, L. Yao, A. J. Tan, P. Agrawal, S. Emori, H. L. Tuller, S. Van Dijken, and G. S. D. Beach, Nat. Mater. **14**, 174 (2015).
[13]M. Kawaguchi, K. Shimamura, S. Ono, S. Fukami, F. Matsukura, H. Ohno, D. Chiba, and T. Ono, Appl. Phys. Express **5**, 063007 (2012).

[14]Y. N. Yan, X. J. Zhou, F. Li, B. Cui, Y. Y. Wang, G. Y. Wang, F. Pan, and C. Song, Appl. Phys. Lett. **107**, 122407 (2015).
[15]K. Shimamura, D. Chiba, S. Ono, S. Fukami, N. Ishiwata, M. Kawaguchi, K. Kobayashi, and T. Ono, Appl. Phys. Lett. **100**, 122402 (2012).
[16]M. Jiang, X. Z. Chen, X. J. Zhou, B. Cui, Y. N. Yan, H. Q. Wu, F. Pan, and C. Song, Appl. Phys. Lett. **108**, 202404 (2016).
[17]T. Maruyama, Y. Shiota, T. Nozaki, K. Ohta, N. Toda, M. Mizuguchi, A. A. Tulapurkar, T. Shinjo, M. Shiraishi, S. Mizukami, Y. Ando, and Y. Suzuki, Nat. Nanotechnol. **4**, 158 (2009).
[18]X. Zhou, Y. Yan, M. Jiang, B. Cui, F. Pan, and C. Song, J. Phys. Chem. C **120**, 1633 (2016).
[19]N. Di, J. Kubal, Z. Zeng, J. Greeley, F. Maroun, and P. Allongue, Appl. Phys. Lett. **106**, 122405 (2015).
[20]W. Stoecklein, S. S. Parkin, and J. C. Scott, Phys. Rev. B **38**, 6847 (1988).
[21]D. Atkinson, D. A. Allwood, G. Xiong, M. D. Cooke, C. C. Faulkner, and R. P. Cowburn, Nat. Mater. **2**, 85 (2003).
[22]R. P. C. D. A. Allwood, G. Xiong, C. C. Faulkner, D. Atkinson, and D. Petit, Science **309**, 1688 (2005).
[23]M. Hayyan, F. S. Mjalli, M. A. Hashim, I. M. AlNashef, and T. X. Mei, J. Ind. Eng. Chem. **19**, 106 (2013).
[24]T. Fujimoto and K. Awaga, Phys. Chem. Chem. Phys. **15**, 8983 (2013).
[25]T. Liu, R. Vilar, S. Eugénio, J. Grondin, and Y. Danten, J. Appl. Electrochem. **45**, 87 (2015).
[26]S. P. Ong, O. Andreussi, Y. Wu, N. Marzari, and G. Ceder, Chem. Mater. **23**, 2979 (2011).
[27]D. A. Allwood, G. Xiong, M. D. Cooke, and R. P. Cowburn, J. Phys. D: Appl. Phys. **36**, 2175 (2003).
[28]C. Bi, Y. Liu, T. Newhouse-Illige, M. Xu, M. Rosales, J. W. Freeland, O. Mryasov, S. Zhang, S. G. E. Te Velthuis, and W. G. Wang, Phys. Rev. Lett. **113**, 267202 (2014).
[29]M. Fitzsimmons, T. Silva, and T. Crawford, Phys. Rev. B **73**, 014420 (2006).
[30]J. P. Nibarger, R. Lopusnik, Z. Celinski, and T. J. Silva, Appl. Phys. Lett. **83**, 93 (2003).
[31]M. C. Biesinger, B. P. Payne, A. P. Grosvenor, L. W. M. Lau, A. R. Gerson, and R. S. C. Smart, Appl. Surf. Sci. **257**, 2717 (2011).
[32]M. C. Biesinger, B. P. Payne, L. W. M. Lau, and R. S. C. Smart, Surf. Interface Anal. **41**, 324 (2009).
[33]M. Salou, B. Lescop, S. Rioual, A. Lebon, J. Ben Youssef, and B. Rouvellou, Surf. Sci. **602**, 2901 (2008).